Journal of Controlled Release 254 (2017) 44–54

Contents lists available at ScienceDirect

Journal of Controlled Release

journal homepage: www.elsevier.com/locate/jconrel

Enhanced topical penetration, system exposure and anti-psoriasis activity of two particle-sized, curcumin-loaded PLGA nanoparticles in hydrogel

Lin Sun[a], Zeyu Liu[a], Lun Wang[a], Dongmei Cun[b], Henry H.Y. Tong[c], Ru Yan[a], Xin Chen[a], Ruibing Wang[a], Ying Zheng[a,*]

[a] State Key Laboratory of Quality Research in Chinese Medicine, Institute of Chinese Medical Sciences, University of Macau, Macao SAR, China
[b] Department of Pharmaceutical Sciences, Shenyang Pharmaceutical University, 103 Wenhua Road, Shenyang 110016, Liaoning, China.
[c] School of Health Sciences, Macao Polytechnic Institute, Macao SAR, China

ARTICLE INFO

Keywords:
Curcumin
PLGA nanoparticle
Penetration
Psoriasis-like mouse model
Topical drug delivery

ABSTRACT

Psoriasis is an immune-mediated skin disorder, which is triggered by the aberrant activation of dendritic cells in skin. This activation is followed by the complex interaction between the immune cells in the skin and keratinocyte in the epidermis. To improve the conditions of poor aqueous solubility and chemical stability, overcome skin barriers, and enhance *in vivo* anti-psoriatic activity, curcumin (Cur) loaded poly (lactic-*co*-glycolic acid) (PLGA) nanoparticles (NPs) were fabricated and administered by topical route to treat imiquimod (IMQ)-induced psoriasis-like mouse model. Spherical Cur-NPs with the mean particle sizes of 50 nm and 150 nm, respectively, were fabricated using a multi-inlet vortex mixer system, with both exhibiting significantly stronger anti-proliferation effect than Cur solution on HaCaT cells *in vitro*. Psoriatic skin was utilized in the *in vitro* skin penetration studies, and the results demonstrated that more drugs penetrated through or accumulated in the skin when administered as the Cur-NPs-loaded hydrogel compared to the drug suspension loaded hydrogel. To compare the nanosizing effect of these Cur-NPs, the mice with IMQ-induced psoriasis-like skin disease were treated with blank gel, Cur gel, 50 nm sized NPs gel, 150 nm sized NPs gel or tracrolimus cream (positive control), respectively. The results indicated that Cur-NPs hydrogel has a superior performance to Cur hydrogel on the IMQ-induced psoriasis-like mouse model in terms of morphological evaluation, biomarkers at mRNA, and protein levels. In conclusion, encapsulation of Cur into PLGA NPs, particularly for NPs of 50 nm, could facilitate lipophilic Cur's dispersion, sustained-release, accumulation, and penetration across the skin and into the blood circulation, which significantly improves anti-psoriasis activity in mice.

1. Introduction

Psoriasis is an immune-mediated inflammatory disease, which affects up to 2% of the population all over the world [1]. The patients frequently suffer from scaly, itchy, painful, plaque-like and disfiguring skin lesions during their lifetime. Several in-house and environmental stimuli, including trauma, infection, or certain drugs, can trigger the progress of psoriasis, although the exact mechanism remains unclear. It is generally believed that aberrant activation of dendritic cells in the skin, which results in the subsequent complex interactions between the cells in immune system and keratinocytes, is responsible for the initiation of psoriasis pathogenesis [2]. The interleukin-23 (IL-23)/IL-17 cytokine axis plays a critical role in the pathogenesis of psoriasis [3]. The activated dendritic cell in skin release IL-12 and IL-23, leads to differentiation of helper T cell (Th) 1 and Th 17 cells, which release Th1 and Th17 cytokines including IL-17 and IL-23. During this procedure, IL-23, IL-17, IL-22, IL-1β, IL-6, and TNF-a interact as a network, followed with further activation of keratinocytes and induction of the proliferation of keratinocytes. At present, topical treatments, systemic medications, and phototherapy are the three main methods to treat psoriasis. It is highly recommended that the 90% of psoriasis patients who are affected by either mild or moderate psoriasis [4] take topical treatment with low systemic toxicity and potential targeting ability towards the affected skin. Biological agents used for systemic therapy in severe cases of psoriasis demonstrated a systemic toxicity and high cost. Rapid growth of new cells in psoriatic skin could be slowed down by phototherapy, which is used as a supplementary treatment for the other two methods.

Curcumin (Cur), a hydrophobic ingredient of turmeric, is widely considered to be as an effective agent for wound healing, asthma, epilepsy, and cancer [5]. As a selective phosphorylase kinase inhibitor, Cur also has been reported as a promising anti-psoriatic agent used in

* Corresponding author at: Institute of Chinese Medical Sciences, University of Macau, 6/F, Rm 6010, N22, Macao, China.
E-mail address: yzheng@umac.mo (Y. Zheng).

http://dx.doi.org/10.1016/j.jconrel.2017.03.385
Received 18 November 2016; Received in revised form 27 February 2017; Accepted 23 March 2017
Available online 24 March 2017

oral and topical routes [6–8]. It inhibits the IL-23/IL-17A axis and can indirectly down-regulate the IL-17A/IL-22 expression in the psoriatic skin [9]. Although Cur has demonstrated bioactivity on psoriasis treatment [7], its poor aqueous solubility, chemical stability, and the low penetration ability across the skin restricted its clinical application. Therefore, formulation approaches to improve Cur delivery are desperately needed in topical therapy of psoriasis.

Nanotechnology has been applied in the topical treatment of immune-related skin diseases since the early 1980s [10]. Due to the high affinity to skin barriers and good compatibility in loading lipophilic drugs, lipid-based and polymeric nanoparticles (NPs) have been developed to improve drug penetration and therapeutic efficacy, or to reduce the toxicity of the active agents [11]. Poly (lactic-*co*-glycolic acid) (PLGA) is an FDA approved biodegradable copolymer, which is used to fabricate nanoparticles with sustained drug release and good compatibility. Although encapsulation of drug, as the nanoparticles have demonstrated, enhanced topic delivery of drugs with enhanced therapeutic efficacy, the mechanism of NPs' penetration has been a controversial topic [12]. It is generally accepted that the NPs will accumulate and penetrate through the follicle's orifices of the intact skin, which accounts for 0.1% of the skin's surface [13]. As the outermost layer of the skin, *stratum corneum* plays a key role in maintaining the internal environment and providing protection from foreign agents leading to diseases. The occurrence of psoriasis could induce the changes in the morphological and physiological functions of the skin, which may alter barrier function of *stratum corneum* and then change the penetration behavior of active agents and their formulations. Previously, NPs have shown promising results in enhancing the drug delivery into the normal skin [12]. However for the psoriatic skin with a fragile organization of *stratum corneum* [14], the changes in penetration behavior of NPs have not been fully investigated. Therefore, in this work, imiquimod (IMQ)-induced psoriatic skin will be utilized to evaluate the NPs penetration *in vitro*.

Taking Curcumin as the lipophilic model drug, two particle-sized Cur-loaded PLGA NPs have been fabricated in the present work to investigate their *in vitro* release behavior, anti-proliferation activity on HaCaT cell line, permeation across the skin barriers into the circulation system, and anti-psoriasis activity on IMQ-induced psoriasis-like mouse model.

2. Materials and methods

2.1. Materials

Curcumin was obtained from Yung Zip Chemical Industries Ltd. (Taiwan), while PLGA (50:50 LA:GA (w:w), 5000 Da) was purchased from Wako Pure Chemical Industries Ltd. (Japan). Polyvinylpyrrolidone (PVP) was obtained from Wing Hing Chemical Company Ltd. (BP grade, Hong Kong). Carbopol 974 was supplied by Chineway (Shanghai, China). IMQ was purchased as Aldara, a topical cream (5% imiquimod; Health Care Limited, Loughborough UK). Protopic (0.1%, tacrolimus) was purchased from Astellas Pharma Tech Co., Ltd. (Toyama, Japan). Paraformaldehyde (4%) was obtained from Jingxin Biological Technology (Guangzhou, China). Methanol and acetonitrile (ACN) were attained from Merck (Darmstadt, Germany). Milli-Q water was collected from a Millipore Direct-Q ultra-pure water system (Millipore, Bedford, USA). Absolute ethanol was purchased from Tianjin Kaitong Chemical Reagent Co. Ltd. (Tianjin, China).

2.2. Cell line and cell culture

The HaCaT human keratinocyte cell line was kindly supplied by Dr. Yu Hua at the Institute of Chinese Medical Sciences, University of Macau. Cells were cultured in Dulbecco's modified Eagle's (DMEM) medium with 5% (v/v) fetal bovine serum (FBS, Life Technologies, New York, USA), L-glutamine of 2 mM and penicillin/streptomycin (100 IU/mL/100 μg/mL) at 37 °C in the presence of 5% CO_2, and 95% relative humidity. The growth media was replaced every 2 days.

2.3. Animals

Female C57/BL6 mice (7–9 weeks old) were supplied and housed under specific pathogen-free conditions by the Experimental Animal Center of Faculty of Health Sciences, University of Macau (Macau, China). The University of Macau Animal Ethics Committee approved all the used animal protocols. All experiments were carried out in accordance with the NIH Guidelines for the Care and Use of Laboratory Animals. All efforts were made to minimize animal suffering and to limit the number of animals used.

2.4. Preparation of Cur-NPs

Cur-PLGA NPs were formulated using a conventional anti-solvent method and flash precipitation method that we previously developed [15]. Briefly, Cur and PLGA were dissolved (1:1, w/w, 5 mg/mL) in dimethylformamide (DMF) to form the organic phase, while PVP (0.8 mg/mL) was chosen as the stabilizer in the aqueous phase. Organic phase of 4 mL was injected into 20 mL aqueous phase (1:5, v/v) with stirring. A multi-inlet vortex mixer (MIVM), consisting of four inlet streams, was used to fabricate small-sized Cur-NPs. One of the inlet streams was 1 mL organic phase with the same composition described above, and one inlet stream consisted 9 mL aqueous solution of PVP at a concentration of 0.4 mg/mL. The other two streams were both Milli-Q water. The pump (Harvard Apparatus, PHD 2000, USA) speed was 10:90 mL/min (organic phase and one of the Milli Q channel: aqueous phase with PVP and one of the Milli Q channel). After the fabrication, the organic solvent and non-encapsulated free Cur was removed from the suspension by a dialysis bag with the molecular weight cut-off 3.5 kDa in Milli-Q water for 24 h in dark place.

2.5. Characterization of Cur-NPs

The size distribution of the NPs was measured by dynamic light scattering (DLS, Nano-Zetasizer, Malvern, UK). Measurements were carried out in triplicate for each sample. According to a previous report [16], an ultrafiltration method was used to calculate the encapsulation efficiency of the Cur-NPs. Briefly, an NPs suspension was placed in the inner tube of an ultrafiltration tube (Amicon Ultra-4 Centrifugal Filter Unit, 10 kDa cutoff). After centrifugation (4000 × *g*, 20 min), the filtrate containing unformulated Cur in the outer tube was collected. The total concentration (unfiltered suspension) and filtrate were determined using HPLC. The HPLC conditions are described in Section 2.10.1, while the calculation method of encapsulation efficiency (EE%) and drug loading capacity were calculated using the following equations:

$$\text{Encapsulation efficiency\%} = \frac{\text{Unfiltered drug} - \text{free drug in filtrate}}{\text{Unfiltered drug}} \times 100\% \quad (1)$$

$$\text{Drug loading capacity\%} = \frac{\text{Drug}}{\text{Drug} + \text{polymeric agent}} \times \text{EE} \times 100\% \quad (2)$$

The morphology of Cur-NPs was examined by transmission electron microscopy (TEM, Hitachi TEM system, Japan) at an accelerating voltage of 80 kV. In short, one drop of the Cur-NP suspension was placed on the surface of a copper grid for approximately 1 min, and subsequently the excess solution was removed by filter paper. For structural characterization, 2% (w/v) neutral phosphotungstic acid was used to negatively stain the copper grid. After the sample was air-dried for 20 min, the samples were analyzed by TEM.

The *in vitro* release profile of Cur and Cur-NPs was investigated in phosphate-buffered saline (PBS, pH 7.4) for 72 h in a dark location at

32 °C. The specific method was performed according to the procedure described in previous reports [17], which demonstrated that the free Cur would degrade immediately under the condition of pH 7.4. Therefore the drug residue in nano-suspension could be considered as the unreleased Cur. Released drug was calculated as: $(Drug_{total} - Drug_{Residue}) / Drug_{total} \times 100\%$. Experiments were performed in triplicates.

2.6. Apoptosis of HaCaT cells

The effect of Cur in different formulations on apoptosis induction in HaCaT cells was determined using the FITC Annexin V Apoptosis Detection Kit I (BD Pharmingen, San Diego, USA) and analyzed by flow cytometry (FACS CantoTM, BD Bioscience, Franklin Lakes, NJ, USA). HaCaT cells of 4×10^5 were seeded and incubated with Cur or Cur-NPs (30 μM) in 12-well plates. After 24 h, the cells were washed with PBS. Cell apoptosis test was performed according to the manufacturer's instructions provided with the kit. The cells were later analyzed by flow cytometry. The experiments were performed in triplicate. The percentage of apoptosis was calculated by adding the average value of early and late apoptosis rate.

2.7. Preparation of drug loaded hydrogel

Topical formulations should have adequate viscosity to be applied onto the skin. Carbopol was chosen as the matrix of the Cur-loaded NPs. Carbopol of 1% (w/v) was slowly added into the suspension of Cur-loaded NPs, with slow constant stirring in darkness for 24 h. After adequate swelling, the gel was neutralized to pH 6 by drop-wised addition of triethanolamine. For free drug-loaded gel, Cur was added into the blank Carbopol gel, which was prepared by combining triethanolamine and propylene glycol. The drug concentration (~0.25 mg/mL) was determined by HPLC before use.

2.8. In vitro skin permeation studies

2.8.1. Psoriatic skin preparation

The skin preparation was performed according to the procedure described in previous report with modifications [18]. The induction process of psoriatic skin on mice backs is described in Section 2.9.1. After the model establishment, female C57/BL6 mice were anesthetized using chloral hydrate (4%, 0.1 mL/10 g, i.p.) and shaved carefully using a clipper and an electrical shaver. Full skin was excised after the mice had been sacrificed by the inhalation of CO_2. The integrity of the skin was attentively checked with microscopy. Any skin that was not complete was rejected. After removing the subdermal tissue, the skin was washed with physiological saline, and then stored at − 80 °C until required. Before use, the skin was thawed to room temperature.

2.8.2. Penetration studies

Psoriatic mouse skin was mounted on Franz cell (PermeGear V6-CA, US) with the *stratum corneum* facing up. The capacity of donor and receiver parts was 2.0 mL and 8.0 mL, respectively, while the effective diffusion area was 1 cm^2. The two cells were clamped securely using a clip and connected to a water bath at 32 °C, which is the temperature of human skin. Different formulations in gel (2 mL, 0.25 mg/mL) were added in the donor cells, while 20% ethanol-water (8 mL) was added to the acceptor cells with continuous stirring to maintain sink conditions. A sample of 1 mL was withdrawn from acceptor cells and supplemented with fresh receptor solution at predetermined intervals. The effective diffusion area of skin sample was washed with fresh receptor solution three times and wiped. The skin was then cut into pieces and under ultrasonic extraction for 30 min in 80% aqueous acetonitrile. After centrifugation (12,500 × *g*, 10 min), the sample was measured with LC-MS/MS using emodin as the IS. The drug accumulation in the skin and its penetration amount were calculated, which was obtained from the measured concentration and volume of the receiver phase. The transdermal penetration curve was plotted as the cumulative amount of drug permeated per unit area (*Q*) collected in the receiver compartment as a function of time [18]. The experiments were performed in triplicates.

2.9. In vivo studies

2.9.1. Establishment of IMQ-induced psoriasis-like mouse model

IMQ is a TLR7/8 ligand and a potent immune activator. The topical application of IMQ can induce and exacerbate psoriasis [19]. Fits et al. provided a modified procedure to develop the psoriasis-like mouse model [20]. Female C57BL/6 mice were utilized and divided into 6 groups ($n = 6$), which were all treated with IMQ (62.5 mg of commercially available IMQ cream (5%), corresponding to a daily dose of 3.125 mg of the active compound) on the shaved back and right ear every 24 h for 7 days. In addition to the negative control group (IMQ treatment only), the inflamed skin area of other 5 groups were also treated once daily with blank gel, Cur gel, 50 nm Cur-NPs gel, 150 nm Cur-NPs gel, or tacrolimus cream (0.1%, positive control), respectively. The dose of Cur was 0.25 mg/day/mouse, while the tacrolimus was 0.1 mg/day/mouse.

2.9.2. Histology

The treated dorsal skin was obtained at the end of the experiment, and then it was fixed by 4% paraformaldehyde. After they had been embedded in paraffin, 4 μm microtome sections of skin were deparaffinized, rehydrated, and stained with hematoxylin and eosin (H & E). A microscope (BDS 200, Aote, China) equipped with a computer-controlled digital camera was used to visualize the sections.

2.9.3. Psoriasis Area Severity Index (PASI) evaluation.

Based on the clinical Psoriasis Area and Severity Index (PASI) [20], an objective scoring system was developed to evaluate the severity of inflammation on the mice dorsal skins and ears. Three factors showed effects on the PASI, which were erythema, scaling, and thickening. All of these factors were scored independently by two people on a scale from 0 to 4: 0, none; 1, slight; 2, moderate; 3, marked; and 4, very marked. The cumulative score (erythema plus scaling plus thickening) indicated the severity of inflammation (scale 0–12). The scoring was performed every 24 h for 7 days.

2.9.4. Weight ratio of spleen to body (spleen/body wt%).

The spleen is the largest organ in the human immune system [21], with the weight considered to be a sensitive indicator of immune stimulation or depletion. The increased spleen/body wt% may demonstrate the increased amount of cells in the spleen, which reflect the enhancing of the disease related to immune activation [22]. The spleens of the mice were harvested at the end of the experiment, and the spleen/body wt% was measured.

2.9.5. Treatment of skin and blood samples for quantification.

At the end of the experiment, the dorsal skin and blood samples were attained after being sacrificed by the inhalation of CO_2. Skin samples were washed in saline and wiped. Meanwhile, the plasma samples were separated immediately by centrifugation at 1360 × g for 10 min, using a Scilogex D1008E Centrifuge (Eleoption, USA), and stored at − 80 °C until analyzed. The skin was cut into pieces then homogenized by using Tissuelyser II Disruption System (Qiagen, CA, USA). To a 100 mg portion of each homogenized skin sample, 300 μL 80% aqueous acetonitrile was added and sonicated for 30 min. After centrifugation at 13,871 × g (Sorvall Legend Micro 21R, Thermo Scientific, USA) was performed at 4 °C for 10 min, the supernatant was collected. Skin or blood samples were mixed with internal standard (IS) solution (100 ng/mL emodin dissolved in acetonitrile) at the ratio of 1:2, v/v. After centrifuging was performed at 21,100 × g at 4 °C for

Table 1
Primer sequences of mouse genes examined by quantitative real-time PCR.

Primer	Base sequence (5'to3')
IL-1β (S)	CCCTGCAGCTGGAGAGTGTGGA
IL-1β (AS)	TGTGCTCTGCTTGTGAGGTGCTG
IL-6 (S)	CCTCTCTGCAAGAGACTTCCAT
IL-6 (AS)	AGTCTCCTCTCCGGACTTGT
IL-17F (S)	ACCCGTGAAACAGCCATGGTCAAG
IL-17F (AS)	CCCATGGGGAACTGGAGCGG
IL-22 (S)	CAGCTCCTGTCACATCAGCGGT
IL-22 (AS)	AGGTCCAGTTCCCCAATCGCCT
IL-23 (S)	TCCTCCAGCCAGAGGATCACCC
IL-23 (AS)	AGAGTTGCTGCTCCGTGGGC
TNF-α (S)	GCCCACGTCGTAGCAAACCAC
TNF-α (AS)	GCAGGGGCTCTTGACGGCAG
IFN-γ (S)	TAACTCAAGTGGCATAGATGTGGAAG
IFN-γ (AS)	GACGCTTATGTTGTTGCTGATGG
STAT3 (S)	GAAGCCGACCCAGGTGC
STAT3 (AS)	GTCACGTCTCTGCAGCTTCT
GAPDH (S)	GGGCTCTCTGCTCCTCCCTGT
GAPDH (AS)	CGGCCAAATCCGTTCACACCG

10 min, 10 μL of each sample or standard was analyzed using LC/MS/MS.

2.9.6. Quantitative real-time PCR (qRT-PCR).

Total RNA was harvested from the 100 mg mice skin with 1 mL Trizol (Invitrogen, USA) as per the manufacturer's protocol. Tissuelyser II Disruption System (Qiagen, CA, USA) was used for homogenization, with the conditions of 30 frequency/s 10 min. The isolated RNA was reverse transcribed into cDNA with PrimeScript RT Reagent Kit (Takara, Japan) and GeneAmp PCR System 9700 (Thermo Fisher Scientific, USA). The operation was performed according to the manufacturer's instructions, and the reaction proceeded at 37 °C for 15 min, then at 85 °C for 5 s, then at 4 °C.

To validate the amplifications, qRT-PCR was performed using the SYBR Premix Ex Taq II (Takara, Japan) on Mx3005P QPCR Systems (Agilent Technologies, USA). The operation was carried out according to the manufacturer's instructions, while the sequences of primers are shown in Table 1. GAPDH was chosen as the housekeeping gene. The relative mRNA levels were calculated using the comparative Ct method (ΔΔCt).

2.9.7. Cytokine measurement using Bio-Plex.

Total protein of mouse skin was extracted from the harvested dorsal skin by 1 mM phenylmethanesulfonyl fluoride added radio immunoprecipitation assay (RIPA) lysis buffer (P0013D, Beyotime Biotechnology, China) and determined using BCA Protein Assay Kit (Tiangen biotech, Beijing, China). IL-12P40, IL-17A, IL-22, TNF-α and IFN-γ were analyzed by using the Bio-Plex™ 200 system (Bio—Rad, USA). The protein concentration was diluted at 200–900 μg/mL with sample diluent being in the kit before the experiment. The specific operation was performed according to the operation instructions of Bio-Plex Cytokine Assay Kit.

2.10. Analytical methods

2.10.1. In vitro quantitative analysis

The encapsulation efficiency of Cur-NPs and the release data of Cur and Cur-NPs were measured using an Agilent 1200 Series HPLC system (Agilent, USA) equipped with a diode array detector (DAD) detector. Analyses were performed using an Agilent Zorbax SB-C18 column (250 mm × 4.6 mm, 5 μm, Agilent) at room temperature. The mobile phase was acetonitrile: 0.1% H_3PO_4 solution (6:4, v/v) at a flow rate of 1 mL/min. The wavelength of the detector was set at 430 nm. The injection volume for all samples was 50 μL.

2.10.2. In vivo quantitative analysis

An ABI 4000 Q-Trap™ hybrid triple quadrupole linear ion trap mass spectrometer (Applied Biosystems, Foster City, CA), with a Turbo V ionization source, was operated in the negative ion mode and coupled to an Agilent 1200 HPLC system (Agilent Technologies, CA, USA). The separation was executed using a C18 reversed-phase column (Zorbax extend C18, 100 × 2.1 mm id, 3.5 μm, Agilent, USA). The flow rate was 0.4 mL/min, while the mobile phase consisted of acetonitrile and 0.1% aqueous formic acid and eluted in a gradient mode. The quantification was performed using a multiple reactions monitoring mode with the transitions of m/z 367.1 → 134.0 for CUR and 268.0 → 225.0 for emodin (IS). The main working parameters were set as follows: ion-spray voltage, − 5500 V; ion source temperature 500 °C; gas 1, 40 psi; and gas 2, 40 psi, and curtain gas, 20 psi. The concentrations of the analyte were determined using the software Analyst 1.5 software (Applied Biosystems, CA, USA).

2.11. Statistical analysis

Results are expressed as the mean ± S.E. The statistical significance of the differences between the treatments was performed *via* one-way or repeated measure ANOVA analysis using SPSS software, where a $p < 0.05$ was considered statistically as significant.

3. Results

3.1. Characterization of Cur-NPs

As shown in Fig. 1A and B, the Cur-NPs with an average particle size of 48.89 ± 0.19 nm (PDI = 0.11 ± 0.01) were fabricated using MIVM, while the larger Cur-NPs with an average particle size of 152.00 ± 1.39 nm (PDI = 0.10 ± 0.01) were prepared using the conventional anti-solvent precipitation method described in section 2.4. The encapsulation efficiency for 50 nm and 150 nm sized Cur-NPs was 96.45 ± 1.53% and 92.48 ± 0.14%, respectively, while the drug loading capacity for 50 nm and 150 nm sized Cur-NPs was 48.23 ± 0.77% and 46.24 ± 0.07%, respectively. All the fabricated NPs showed a spherical shape without visible aggregation among the particles, which is consistent with the results obtained from DLS measurements.

In Fig. 1C, the cumulative release of Cur from Cur-NPs is > 85% within 72 h, whereas the complete drug release was observed within 8 h from unformulated Cur suspension under the sink conditions. All the fabricated Cur-NPs showed a sustained-release behavior, where the small sized NPs released faster ($p < 0.05$) in 48 h. The preliminary burst of drug was from the Cur absorbed on the surface of the PLGA NPs, while the others were entrapped in the core of PLGA NPs.

3.2. Apoptosis of HaCaT cells

The effect of Cur and Cur-NPs on HaCaT cell apoptosis was determined by the FACS flow cytometry with the results summarized in Fig. 2. After exposure to unformulated Cur or two sized Cur-NPs of 30 μM for 24 h, the percentages of early and late apoptotic cells were significantly improved in the NPs treatment groups, which were 14.12 ± 1.06% for 50 nm and 11.08 ± 0.17% for 150 nm Cur-NPs, respectively. The percentages observed among the Cur group and the blank group were 6.74 ± 0.13% and 4.50 ± 0.20%, correspondingly.

3.3. In vitro skin permeation studies

The *in vitro* transdermal permeability of Cur gel (free drug), 50 nm Cur-NPs gel, and 150 nm Cur-NPs gel through excised psoriatic mouse skin was investigated using Franz diffusion cells. The amount of drugs accumulated during 24 h (Q_{24}) and the drug concentrations in the skin were determined and are summarized in Table 2, while the cumulative

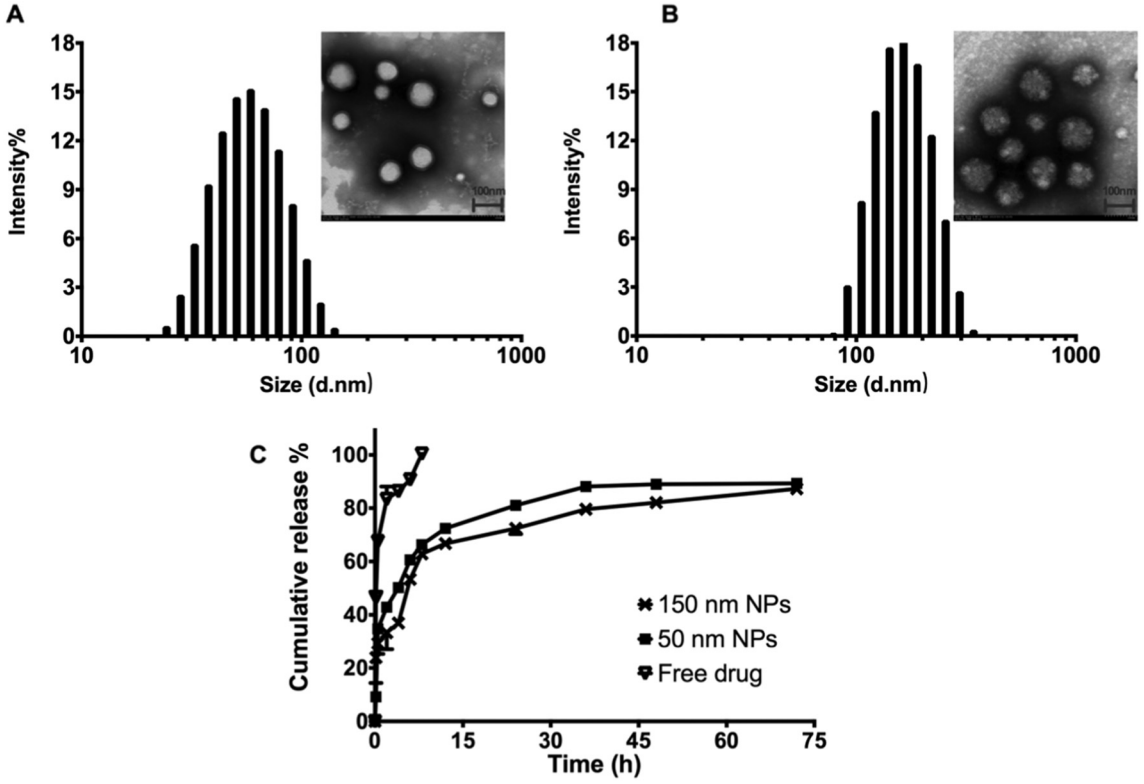

Fig. 1. Particles distribution and TEM image of curcumin (Cur) loaded PLGA nanoparticles (NPs), 50 nm sized (A) and 150 nm sized (B). The bar is 100 nm. Cur release profiles *in vitro* in PBS pH 7.4 at 32 °C (C). Data points shown are mean ± SD (n = 3).

permeation profiles of Cur from the three formulations are shown in Fig. 3A, all of which presented a linear penetration curve and followed zero-order kinetics after few hours' lag time, suggesting a sustained permeation of Cur from different gels. In addition, the 50 nm sized Cur-NPs in gel showed the fastest steady-state flux, while the lowest flux was from Cur in gel. Compared to free Cur-loaded gel, a much higher Q_{24} and drug accumulation in the skin were obtained for both Cur-NPs loaded gels ($p < 0.05$). Moreover, the penetration of Cur in smaller sized NPs in gel was significantly higher than that of the larger one ($p < 0.05$). Although there was no compelling difference between the results of the 50 nm sized NPs in gel and 150 nm sized NPs in gel, the apparent higher drug accumulation was obtained with the larger sized NPs in gel.

3.4. Histology evaluation

A demonstration of the cutaneous inflammation in seven groups is shown in Fig. 4. Compared to the normal untreated group, serious inflamed skin covered with white, scaly and thicken skin are observed in IMQ treated groups by directed observation on the back of the mice. After co-treatment with different formulations, especially for Tacrolimus and 50 nm Cur-NPs in gel treated groups, thicknesses of the white scales and pink color of the inflamed skin were apparently reduced to some extent. Consistent with the appearance of skin, the hyperplasia of basal and suprabasal keratinocytes were also expressed in the psoriatic skin shown in the H & E staining. In addition, abnormal keratinocyte differentiation with marked hyperkeratosis and parakeratosis (nuclei in the stratum corneum) was detected.

3.5. Psoriasis Area Severity Index (PASI) evaluation

The ear thickness, desquamation, and erythema variation in differently treated groups were scored and summarized in Fig. 5(A–C). The ear thickness of the IMQ only group, IMQ + blank gel group, and IMQ + Cur gel group increased with time. The other three groups treated with IMQ + Cur NPs gel or IMQ + tacrolimus (positive control) slightly increased during the 7-day treatment, indicating that the effect of formulated NPs is better than unformulated Cur group on thickness reducing. On Day 3, desquamation and erythema began to display on the dorsal skin of the mice, except for the mice in the tacrolimus treated group which began to show a slight plaque on Day 5. The scores of desquamation and erythema in IMQ + Cur gel group (2.49 ± 0.28 and 2.02 ± 0.42, respectively) were a little lower ($p < 0.05$) than that of the IMQ only group (3.29 ± 0.29 and 3.02 ± 0.14, respectively), suggesting that the Cur gel treatment had little effect on the IMQ-induced skin inflammation. The 50 nm and 150 nm NPs gel showed lower desquamation score and similar erythema score, compared to the mice in the Cur gel group ($p < 0.05$). The collective PASI score of six groups is shown in Fig. 5D. As expected after 7-day treatment, the lowest total PASI score (3.51 ± 0.80) was from the IMQ + tacrolimus treated group, whereas the highest total PASI score (9.60 ± 0.27) was obtained from the IMQ only group. There was a similar effect on the total PASI score of the two NPs-treated groups (4.14 ± 1.25 and 4.08 ± 1.11 for 50 nm and 150 nm NPs gel, respectively) and the IMQ + tacrolimus group ($p > 0.05$). The score of IMQ + Cur gel group fell between the IMQ + NPs groups and the IMQ only group, presenting limited reparation effect on the psoriatic skin.

3.6. Weight ratio of spleen to body (Spleen/body wt%)

As shown in Fig. 6, after the application of IMQ for 7 days, the calculated spleen/body wt% of IMQ only group (1.28 ± 0.19) was approximately three times higher than that of the normal mouse group (0.39 ± 0.05), which indicates an increased number of cells in spleen. In turn, this finding signifies immune activation in the psoriasis-like mouse model. Compared to IMQ only group, all of the spleen/body wt% values of the 5 drug treated groups were reduced to some extent.

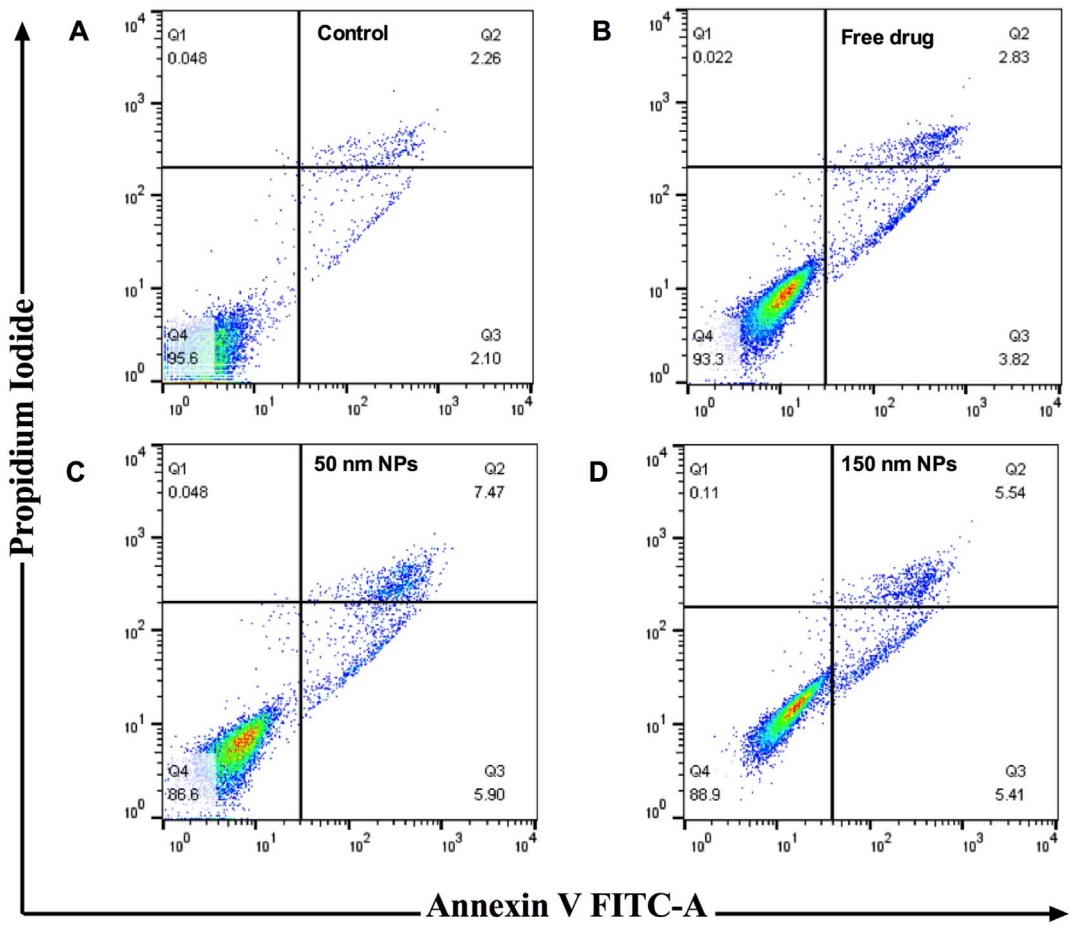

Fig. 2. Analysis of early and apoptotic HaCaT cell after treatment with 30 μM curcumin (Cur) after 24 h by FACS test. A. Normal cell; B. Free drug of Cur; C. 50 nm sized Cur-NPs; D. 150 nm sized Cur-NP.

Table 2
Summary of permeation of Cur from the gel with different formulations through excised psoriatic skin.

Groups	Q_{24} (ng·cm^{-2})	Drug in skin (μg·cm^{-2})
Cur gel	461.19 ± 39.46	1.31 ± 0.25
50 nm NPs gel	1308.70 ± 72.25**	2.90 ± 0.53*
150 nm NPs gel	897.36 ± 88.36*,#	4.41 ± 0.67*

Data are given as mean ± S.E. (n = 3). Q_{24}, penetration amount through skin accumulated during 24 h at 32 °C; Cur, curcumin; NPs, nanoparticles.

* Significantly different from that of Cur gel group (*$p < 0.05$).

** Significantly different from that of Cur gel group (**$p < 0.01$).

Significantly different from that of 50 nm NPs gel group (#$p < 0.05$).

Among these 5 groups, the lowest spleen/body wt% was observed for the tacrolimus treated group. The Cur gel treated group showed a comparable effect to the blank gel treated group, while the two NPs gel treated groups displayed significant decrease on the spleen/body wt% compared to the blank gel ($p < 0.05$). Moreover, there was no apparent difference between the two NPs gel treated groups on spleen/body wt% ($p > 0.05$).

3.7. Determination of Cur in blood and skin using LC-MS/MS

Cur concentration in the mouse blood and skin was determined for the Cur gel and Cur-NPs gel treated groups. As shown in Table 3, the lowest drug concentration in the skin was Cur gel treated mice, while the highest drug concentration was found with the 150 nm NPs gel treated group. With regard to the drug concentration in the circulation, no Cur could be determined after topical administration of Cur gel for 7 days. However, much higher concentrations of Cur were detected in both NPs gel treated groups, where the concentration of the drug after topical administration of mice with small-sized NPs was approximately 5.4 times higher those of the large NPs. This occurrence confirms that small-sized NPs could enhance drug topical penetration across the skin barrier and absorbed into the system circulation to take effect *in vivo*.

3.8. Quantitative real-time PCR (qRT-PCR)

Certain cytokines may play important roles in the pathogenesis and development of psoriasis, which were determined by the mRNA levels using qRT-PCR analysis. The results are summarized in Fig. 7. Compared to the normal mouse group, the mRNA levels of IL-1β, IL-6, IL-17F, IL-22, and IL-23 dramatically increased in the skin of IMQ only group ($p < 0.05$). In contrast, the mRNA levels of these six cytokines significantly decreased in the 50 nm sized Cur-NPs gel group and tacrolimus group compared to the IMQ only group ($p < 0.05$). The application of Cur gel reduced the levels of IL-6, IL-17F, IL-22, and IL-23, while the 150 nm sized Cur-NPs gel group showed a similar effect with the addition of TNF-α. The application of IMQ did not show apparent effects on the levels of IFN-γ and STAT3, whereas the treatment of different gel and cream generally decreased the IFN-γ level.

3.9. Cytokine measurement

As reported before [20], topical application of IMQ will result in the release of a series of inflammatory markers in mouse skin. Therefore,

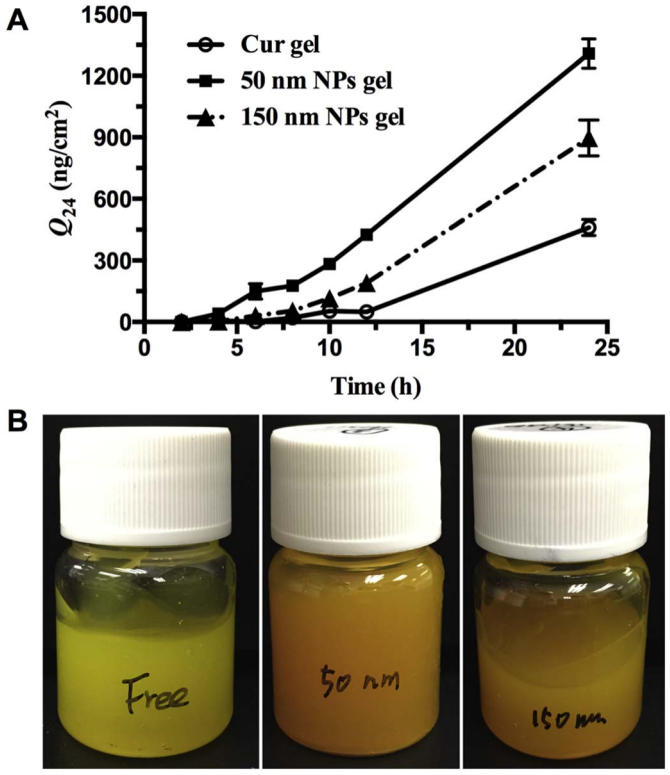

Fig. 3. A. The penetration profiles of Cur gel (free drug), 50 nm Cur-NPs gel, and 150 nm Cur-NPs gel through excised psoriatic mouse skin in 24 h at 32 °C. Data are presented as the mean ± SE, $n = 3$; B. Images of Cur gel (free drug), 50 nm Cur-NPs gel, and 150 nm Cur-NPs gel. Cur, curcumin; NPs, nanoparticles.

five cytokine levels, including IL-12P40, IL-17A, IL-22, TNF-α, and IFN-γ, were determined and summarized in Fig. 8. Compared with the untreated normal mouse group except for IFN-γ (Fig. 8E), the other four cytokines, including IL-12P40, IL-17A, IL-22, and TNF-α, showed a significantly higher level after the treated mouse skin with IMQ cream (Fig. 8A–D, $p < 0.05$). This finding suggests that the application of IMQ promoted the secretion of IL-12P40, IL-17A, IL-22, and TNF-α but did not affect the release of IFN-γ. The Cur treatment groups showed different degrees of inhibition of cytokines release. The 50 nm sized Cur-NPs gel decreased the level of IL-22 and TNF-α significantly ($p < 0.05$), while the 150 nm sized Cur-NPs gel exhibited the best inhibitory effect on the level of IL-12P40. Compared to the Cur gel, the 50 nm sized Cur-NPs gel indicated a more significant inhibitory effect in IL-12P40 and IL-22 protein level of the IMQ-induced psoriasis-like mouse model.

4. Discussion

Transdermal drug delivery systems can be used for the treatment of both systemic and localized diseases. For psoriasis therapy, transdermal delivery is an attractive strategy because of the initiation and progression of the disease that mainly occurs in the skin. In this work, two different sized Cur-loaded PLGA NPs were prepared and evaluated for the topical treatment of psoriasis. To fabricate the smaller Cur-NPs, MIVM was utilized due to the highly efficient mixing of all components in the solvent mixture, inducing an extremely rapid formation of particles [23]. To obtain homogeneous and moderate viscosity of Cur loaded formulations for suitable topical application, Carbopol gel was used as the matrix of Cur and Cur-NPs. The addition of the gel ensured the consistency among the formulations and prolonged the interaction time between the drug and the skin.

To probe the penetration difference between Cur gel and Cur-NPs gel, *in vitro* penetration experiments were performed. In this part, IMQ induced psoriatic skin was used as the penetration barrier. Previous research [24] has indicated that IMQ can disrupt epidermal barrier by reducing involucrin, a cornified-envelope structural protein that dominates barrier function [25], and β-catenin in the upper epidermis, which may induce deficient barrier function. These changes of psoriatic skin may dramatically affect the penetration performance of free drug and Cur in NPs. This occurrence highlights the importance of the

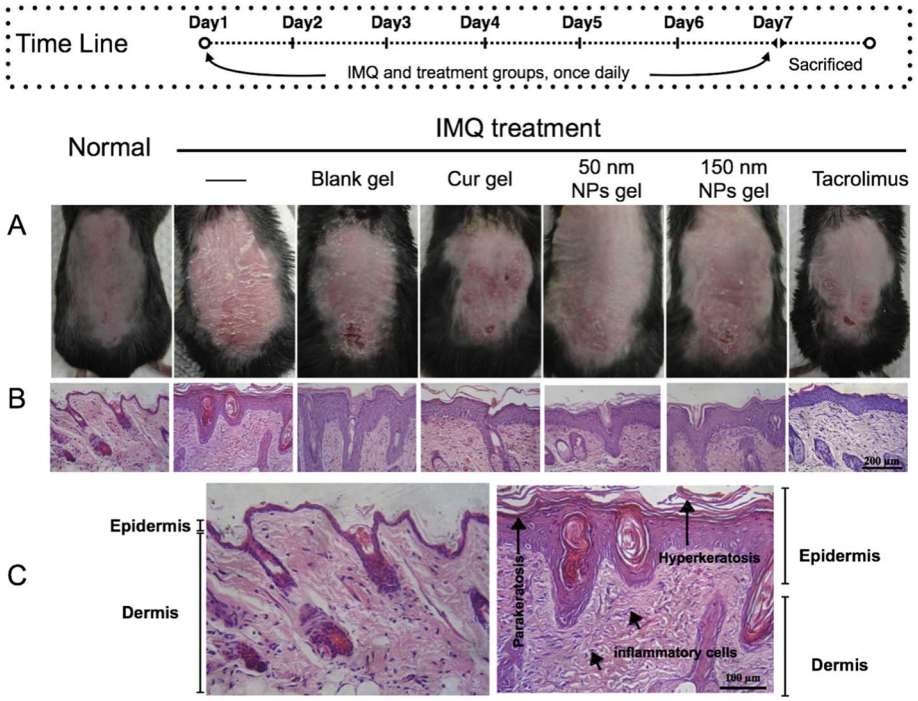

Fig. 4. Topical application of imiquimod (IMQ) induced psoriatic like change on the dorsal skin of mice. At day 7, photographs were taken from the mice (A) and H & E staining (B, bar = 200 μm) was performed to observe the differences of the treatment with blank gel, curcumin (Cur) in gel, 50 nm sized Cur-NPs in gel, 150 nm sized Cur-NPs in gel and tacrolimus cream (positive control). C. Enlarged view of normal mice group (left) and the IMQ only group (right) were also presented for annotation. Bar = 100 μm.

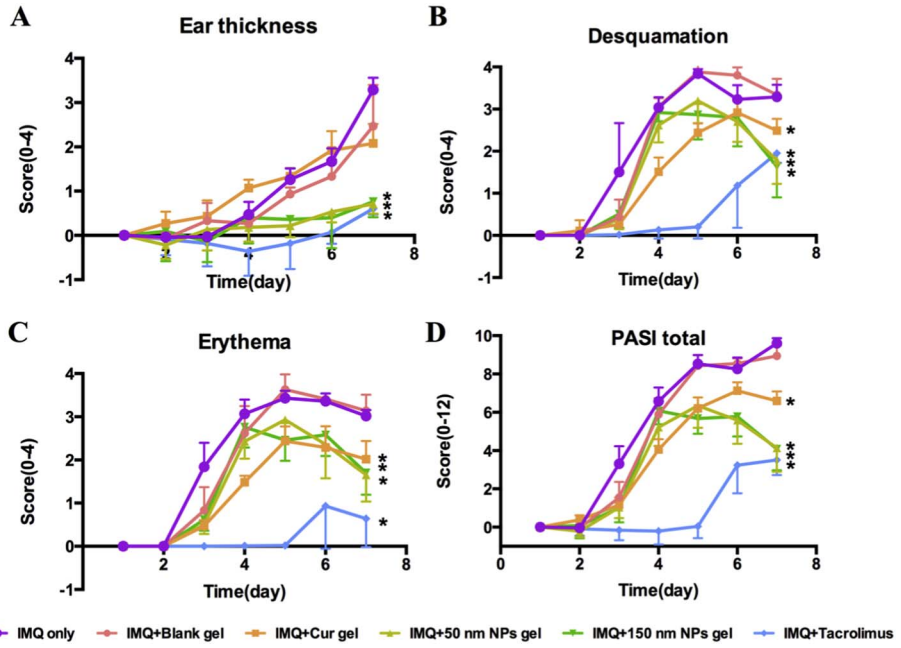

Fig. 5. Psoriasis Area and Severity Index (PASI) scoring of psoriatic dorsal regions of mice in different groups ($n = 6$) were evaluated for 7 days, including erythema, desquamation and thickness of the mouse skin, with a scale from 0 to 4. The total score was from 0 to 12. $^{*}p < 0.05$, compared with IMQ only group ($n = 6$). Cur, curcumin; NPs, nanoparticles.

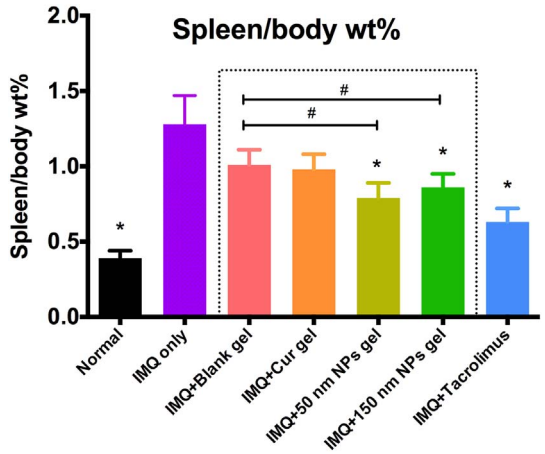

Fig. 6. The ratio of spleen weight to body weight were recorded and calculated at the end of 7 days' application of imiquimod (IMQ) and different treatment in different groups. $^{*}p < 0.05$, compared with IMQ only group, $^{\#}p < 0.05$, compared with blank gel (only compared the groups in which the gel utilized as matrix, $n = 6$). Cur, curcumin; NPs, nanoparticles.

Table 3
In vivo parameters after Cur (0.25 mg/day/mouse, 7d) applied on Imiquimod-induced psoriasis like mice model.

Group of mice	Conc. in skin ($\mu g \cdot g^{-1}$)	Conc. in blood ($ng \cdot mL^{-1}$)
Cur gel	1.24 ± 0.51	ND
50 nm NPs gel	1.93 ± 0.56	17.84 ± 2.09
150 nm NPs gel	4.21 ± 1.08$^{*,\#}$	3.28 ± 1.42$^{\#}$

Data are given as mean ± S.E. ($n = 6$).
ND, not detectable; Cur, curcumin; NPs, nanoparticles.
* Significantly different from that of Cur gel group ($^{*}p < 0.05$)
$^{\#}$ Significantly different from that of 50 nm NPs gel group ($^{\#}p < 0.05$).

pathological membrane on *in vitro* penetration performance, especially for the topical diseases such as psoriasis. The results showed that in comparison with Cur gel, both Cur-NPs gels significantly improved the penetration amount and drug accumulation in the skin. It may be the results of that the PLGA NPs not only as carriers that disperse and protect Cur during delivery but also as a reservoir that could accumulate in the furrows and hair follicles of the skin and then reach to the dermis [12]. The large surface area may also facilitate the longer retention and release of the encapsulated drug in the skin [26].

Compared to Cur gel, both of the developed NPs enhanced drug concentration into the system circulation after topical delivery on the pathological mice skin, which may be due to the free Cur's poor absorption and extensive metabolism *in vivo*. This process is where NPs greatly enhanced its dispersion, release, and penetration, as well as protected drug from rapid metabolism *in vivo*. Both the *in vitro* and *in vivo* results showed that NPs with smaller particle size exhibited higher drug penetration through the pathological skin, and they delivered more drugs into the circulation. Meanwhile, the larger NPs showed more drug retention in the skin with less drug reached to the circulation. Rancan et al. [27] indicated that different NPs can only infiltrate into upper layers of stratum corneum, and penetration into the deeper layers including the viable epidermis and dermis could be achieved when the skin is damaged. However, there was still a restriction on the particle size. During the investigations with four types of NPs with particle sizes of 42 ± 3 nm, 75 ± 6 nm, 190 ± 9 nm, and 291 ± 9 nm, only the 42 ± 3 nm sized NPs could permeate into the deeper skin and exhibit effective interaction with the epidermal cells, such as the dendritic cell which play an important role in the spread of psoriasis [11].

To demonstrate the anti-psoriasis effect on different formulations, HaCaT cell line and IMQ-induced psoriasis-like mouse model were utilized for *in vitro* and *in vivo* studies, respectively. Keratinocyte proliferation is a typical symptom in psoriatic skin, which can be mimicked using HaCaT cell line, an immortal keratinocyte cell line from adult human skin. Cur has been reported presenting the anti-proliferation effect on psoriasis [28], which was also demonstrated in this study. Compared to blank gel group, all the three groups induced apoptosis of HaCaT, in which the two NPs groups presented higher level than Cur group may due to the higher stability of drug in NPs. As a convenient and reasonable model, the IMQ-induced mouse model has been used in several outstanding psoriasis investigations [29,30]. The H & E staining confirmed the formation of plaque psoriasis, which is also evidenced by desquamation, erythema, and thickening of the skin. The Cur-NPs gel dramatically relieved all the symptoms of the psoriatic

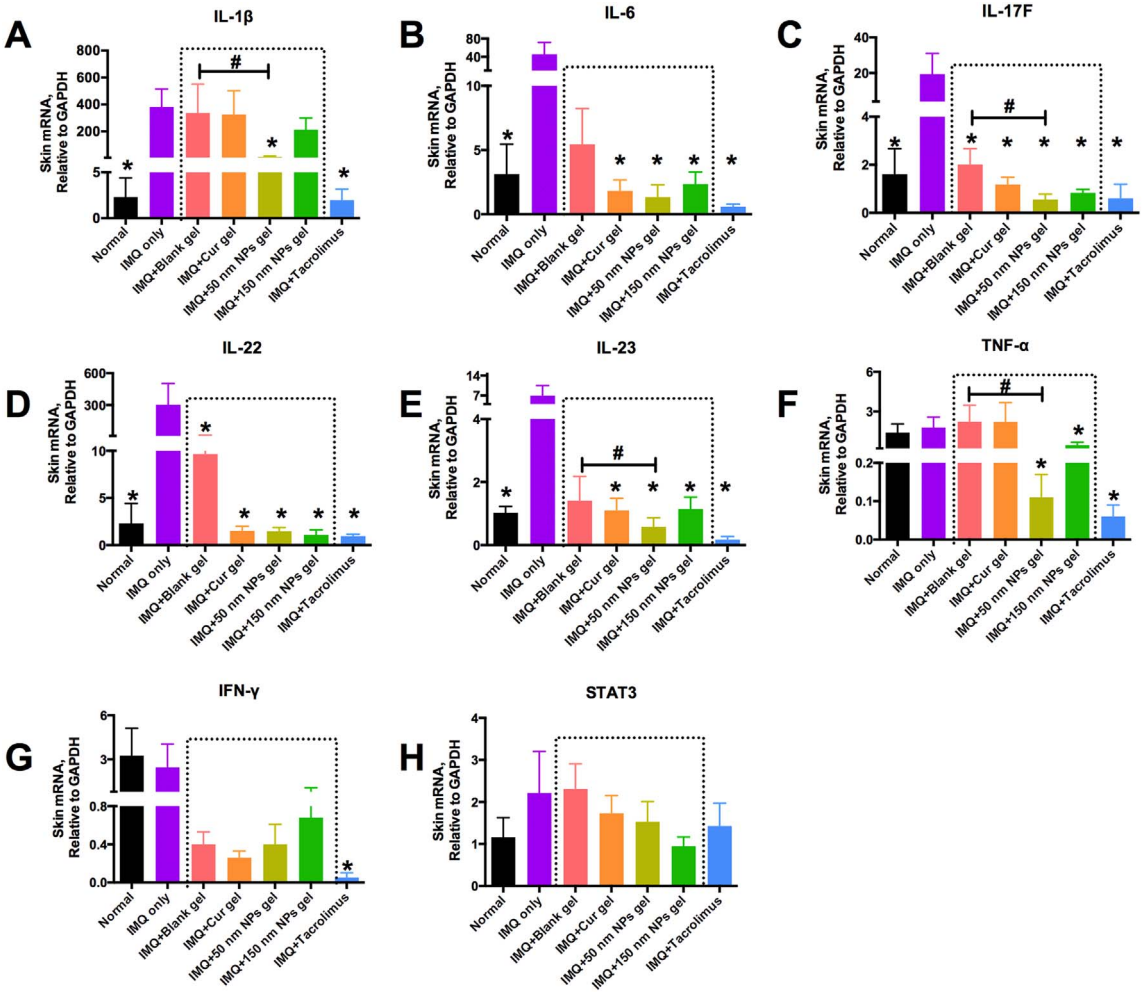

Fig. 7. The mRNA levels of cytokines and differentiation markers in mouse skin treated with different gel or cream. A. IL-1β; B. IL-6; C. IL-17F; D. IL-22; E. IL-23; F. TNF-α; G. IFN-γ; H. STAT3. $^{*}p < 0.05$, compared with IMQ only group, $^{\#}p < 0.05$, compared with blank gel (only compared the groups in which the gel utilized as matrix, $n = 6$). Each value represents the mean and S.E. Cur, curcumin; NPs, nanoparticles.

skin, which was comparable to the positive control, tacrolimus. Additionally, the results of PASI score and the spleen/body wt% indicated a better therapeutic efficacy by the Cur-NPs gel than those treated by the Cur gel.

For the IMQ-induced psoriasis-like mouse model, the IL-23/IL-17 axis plays a crucial role on the exacerbation and development [20]. The mRNA expression and cytokine level of IL-23 and IL-17 would show an enhancement in psoriatic skin. Sun et al. demonstrated that Cur could affect the IL-23/IL-17 axis by inhibiting IL-1β/IL-6, and then indirectly down-regulating IL-17/IL-22 expression [9]. Therefore, the relevant mRNA and cytokines levels were measured using the qRT-PCR analysis and Bio-Plex technique for the mice in different groups. IL-23 is a heterodimeric cytokine composed of an IL-23p19 subunit and IL-12p40 subunit, which is shared with IL-12. Consequently, the evaluation of IL-12p40 in Bio-Plex represented the cytokine level of IL-23. Other biomarkers such as TNF-α and IFN-γ were also tested. IL-17, IL-22, IL-23, and TNF-α cytokines and mRNA levels were significantly lower ($p < 0.05$) in the 50 nm Cur-NPs gel treated group and the positive control, compared to IMQ only and blank gel treated groups. This signifies the effectiveness of the 50 nm Cur-NPs gel and tacrolimus. Compared to the blank gel, the 150 nm Cur-NPs gel showed a significant decrease of IL-12p40 in cytokine level, as well as IL-17 and IL-22 in mRNA levels. Cur gel always showed a similar effect with the blank gel in the cytokines level, both of which exerted little effect in certain cytokines when compared to IMQ-only group. The two gels owe the formation of hydration film on the skin surface treated with the Carbopol matrix gel. The moisture effect of hydrogel could help mitigate some phenomenon of psoriasis and lighten the inflammation development. In these two experiments, the IFN-γ and STAT3 level did not show a significant change after IMQ application, suggesting that they may or may not be less involved in the progress of psoriasis formation in this model. For IL-1β mRNA levels, only 50 nm Cur-NPs gel and tacrolimus showed a significant decrease, in contrast to the group treated by the blank gel, showing less sensitiveness to other Cur loaded formulations.

5. Conclusions

Encapsulation of lipophilic Cur into PLGA NPs have significantly improved bioactivity of Cur on IMQ-induced psoriasis-like mouse model, which benefited from the improved drug dispersion, sustained drug release in PLGA NPs system, enhanced drug penetration, and more effective drug exposure in the skin and circulation. The particle size of the NPs played a considerable role on the topical drug delivery for psoriatic treatment, where drug in smaller particles presented a higher potential to penetrate into the psoriatic skin. The usage of psoriatic skin in the *in vitro* penetration evaluation contributed to the generation of instructive results to *in vivo* study, indicating the importance of pathological barrier during the formulation design and development.

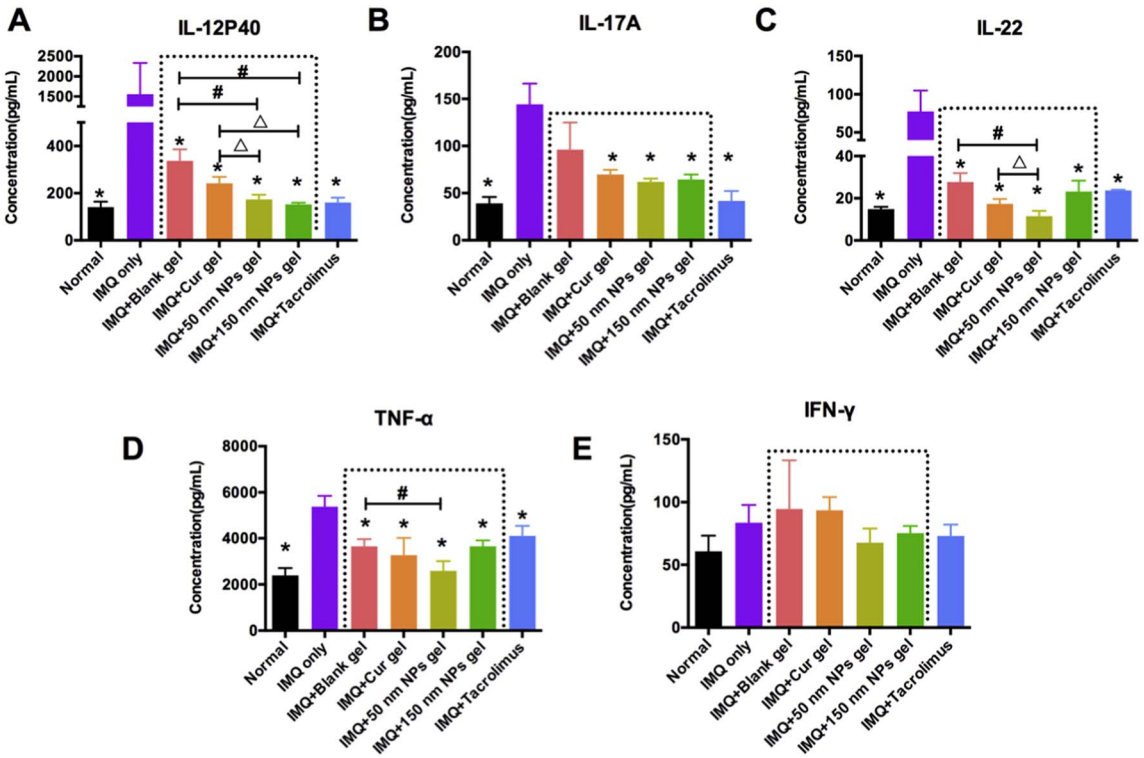

Fig. 8. Cytokine levels of mouse skin in different groups. A. IL-12P40; B. IL-17A; C. IL-22; D. TNF-α; E. IFN-γ. $^{*}p < 0.05$, compared with IMQ only group, $^{\#}p < 0.05$, compared with blank gel (only compared the groups in which the gel utilized as matrix), $^{\triangle}p < 0.05$, compared with Cur gel (only compared the Cur-loaded gel groups), $n = 6$. Each value represents the mean and S.E. Cur, curcumin; NPs, nanoparticles.

Conflict of interest

The authors confirmed that there are no conflicts of interest in this article.

Acknowledgements

This work was supported by a research grant from the University of Macau (No.: MYRG2014-00040-ICMS-QRCM). Authors are thankful to Dr. Zhenping Wang (University of California, San Diego) for enlightening discussion.

References

[1] M. Rahman, S. Akhter, J. Ahmad, M.Z. Ahmad, S. Beg, F.J. Ahmad, Nanomedicine-based drug targeting for psoriasis: potentials and emerging trends in nanoscale pharmacotherapy, Expert Opin. Drug Deliv. 12 (2015) 635–652.
[2] F.O. Nestle, D.H. Kaplan, J. Barker, Mechanisms of disease: psoriasis, N. Engl. J. Med. 361 (2009) 496–509.
[3] Y. Cai, X. Shen, C. Ding, C. Qi, K. Li, X. Li, V.R. Jala, H.G. Zhang, T. Wang, J. Zheng, J. Yan, Pivotal role of dermal IL-17-producing gammadelta T cells in skin inflammation, Immunity 35 (2011) 596–610.
[4] A. Kurian, B. Barankin, Current effective topical therapies in the management of psoriasis, Skin Ther. Lett. 16 (2011) 4–7.
[5] B.B. Aggarwal, C. Sundaram, N. Malani, H. Ichikawa, Curcumin: the Indian solid gold, Adv. Exp. Med. Biol. 595 (2007) 1–75.
[6] T.A. Nguyen, A.J. Friedman, Curcumin: a novel treatment for skin-related disorders, J. Drugs Dermatol. 12 (2013) 1131–1137.
[7] M.C.Y. Heng, M.K. Song, J. Harker, M.K. Heng, Drug-induced suppression of phosphorylase kinase activity correlates with resolution of psoriasis as assessed by clinical, histological and immunohistochemical parameters, Br. J. Dermatol. 143 (2000) 937–949.
[8] D. Kang, B. Li, L. Luo, W. Jiang, Q. Lu, M. Rong, R. Lai, Curcumin shows excellent therapeutic effect on psoriasis in mouse model, Biochimie 123 (2016) 73–80.
[9] J. Sun, Y. Zhao, J. Hu, Curcumin inhibits imiquimod-induced psoriasis-like inflammation by inhibiting IL-1beta and IL-6 production in mice, PLoS One 8 (2013) e67078.
[10] M. Mezei, V. Gulasekharam, Liposomes - a selective drug delivery system for the topical route of administration 0.1. Lotion dosage form, Life Sci. 26 (1980) 1473–1477.
[11] L. Sun, Z. Liu, D. Cun, H.H. Tong, Y. Zheng, Application of nano- and micro-particles on the topical therapy of skin-related immune disorders, Curr. Pharm. Des. 21 (2015) 2643–2667.
[12] T.W. Prow, J.E. Grice, L.L. Lin, R. Faye, M. Butler, W. Becker, E.M.T. Wurm, C. Yoong, T.A. Robertson, H.P. Soyer, M.S. Roberts, Nanoparticles and microparticles for skin drug delivery, Adv. Drug Deliv. Rev. 63 (2011) 470–491.
[13] N. Otberg, H. Richter, H. Schaefer, U. Blume-Peytavi, W. Sterry, J. Lademann, Variations of hair follicle size and distribution in different body sites, J. Invest. Dermatol. 122 (2004) 14–19.
[14] T. Pinheiro, J. Pallon, L.C. Alves, A. Verissimo, P. Filipe, J.N. Silva, R. Silva, The influence of corneocyte structure on the interpretation of permeation profiles of nanoparticles across skin, Nucl. Instrum. Meth. B 260 (2007) 119–123.
[15] Y. Wang, J. Song, S.F. Chow, A.H. Chow, Y. Zheng, Particle size tailoring of ursolic acid nanosuspensions for improved anticancer activity by controlled antisolvent precipitation, Int. J. Pharm. 494 (2015) 479–489.
[16] K.K. Cheng, C.F. Yeung, S.W. Ho, S.F. Chow, A.H.L. Chow, L. Baum, Highly stabilized curcumin nanoparticles tested in an *in vitro* blood-brain barrier model and in Alzheimer's disease Tg2576 mice, AAPS J. 15 (2013) 324–336.
[17] J.B. Sun, C. Bi, H.M. Chan, S.P. Sun, Q.W. Zhang, Y. Zheng, Curcumin-loaded solid lipid nanoparticles have prolonged *in vitro* antitumour activity, cellular uptake and improved *in vivo* bioavailability, Colloid Surf. B 111 (2013) 367–375.
[18] L. Sun, D. Cun, B. Yuan, H. Cui, H. Xi, L. Mu, Y. Chen, C. Liu, Z. Wang, L. Fang, Formulation and *in vitro/in vivo* correlation of a drug-in-adhesive transdermal patch containing azasetron, J. Pharm. Sci. 101 (2012) 4540–4548.
[19] J.K. Wu, G. Siller, G. Strutton, Psoriasis induced by topical imiquimod, Australas. J. Dermatol. 45 (2004) 47–50.
[20] L. van der Fits, S. Mourits, J.S.A. Voerman, M. Kant, L. Boon, J.D. Laman, F. Cornelissen, A.M. Mus, E. Florencia, E.P. Prens, E. Lubberts, Imiquimod-induced psoriasis-like skin inflammation in mice is mediated via the IL-23/IL-17 axis, J. Immunol. 182 (2009) 5836–5845.
[21] A.P. de Porto, A.J. Lammers, R.J. Bennink, I.J. ten Berge, P. Speelman, J.B. Hoekstra, Assessment of splenic function, Eur. J. Clin. Microbiol. Infect. Dis. 29 (2010) 1465–1473.
[22] M.F. Cesta, Normal structure, function, and histology of the spleen, Toxicol. Pathol. 34 (2006) 455–465.
[23] S.F. Chow, C.C. Sun, A.H.L. Chow, Assessment of the relative performance of a confined impinging jets mixer and a multi-inlet vortex mixer for curcumin nanoparticle production, Eur. J. Pharm. Biopharm. 88 (2014) 462–471.
[24] Y.K. Lin, S.H. Yang, C.C. Chen, H.C. Kao, J.Y. Fang, Using imiquimod-induced psoriasis-like skin as a model to measure the skin penetration of anti-psoriatic drugs, PLoS One 10 (2015).
[25] K.H. Hanel, C. Cornelissen, B. Luscher, J.M. Baron, Cytokines and the skin barrier, Int. J. Mol. Sci. 14 (2013) 6720–6745.
[26] K. Tomoda, H. Terashima, K. Suzuki, T. Inagi, H. Terada, K. Makino, Enhanced transdermal delivery of indomethacin-loaded PLGA nanoparticles by iontophoresis, Colloids Surf. B: Biointerfaces 88 (2011) 706–710.

[27] F. Rancan, Q. Gao, C. Graf, S. Troppens, S. Hadam, S. Hackbarth, C. Kembuan, U. Blume-Peytavi, E. Ruhl, J. Lademann, A. Vogt, Skin penetration and cellular uptake of amorphous silica nanoparticles with variable size, surface functionalization, and colloidal stability, ACS Nano 6 (2012) 6829–6842.
[28] A. Pol, M. Bergers, J. Schalkwijk, Comparison of antiproliferative effects of experimental and established antipsoriatic drugs on human keratinocytes, using a simple 96-well-plate assay, In Vitro Cell Dev. Biol. Anim. 39 (2003) 36–42.
[29] C.H. Boakye, K. Patel, R. Doddapaneni, A. Bagde, S. Marepally, M. Singh, Novel amphiphilic lipid augments the co-delivery of erlotinib and IL36 siRNA into the skin for psoriasis treatment, J. Control. Release 246 (2016) 120–132.
[30] P.P. Shah, P.R. Desai, A.R. Patel, M.S. Singh, Skin permeating nanogel for the cutaneous co-delivery of two anti-inflammatory drugs, Biomaterials 33 (2012) 1607–1617.